ACS EARTH AND SPACE CHEMISTRY

http://pubs.acs.org/journal/aesccq

Article

Effect of Concentration, Cooling, and Warming Rates on Glass Transition Temperatures for $NaClO_4$, $Ca(ClO_4)_2$, and $Mg(ClO_4)_2$ Brines with Relevance to Mars and Other Cold Bodies

Ardith D. Bravenec* and David C. Catling

Cite This: *ACS Earth Space Chem.* 2023, 7, 1433−1445

Read Online

ACCESS | Metrics & More | Article Recommendations

ABSTRACT: The hygroscopic and supercooling properties of perchlorates make them potentially important for sustaining liquid water on Mars. To understand the possibility for supercooled liquids and glasses on Mars and other cold bodies, we have characterized the supercooling and vitrification features using differential scanning calorimetry for Na, Ca, and Mg perchlorate brines in a temperature range relevant to Mars. Results show that the glass transition temperature (T_g) depends on the salt composition, concentration, and cooling or warming rate. The difference in T_g may be significant even in a single composition, producing glass transitions with over 40 K difference. A new model was developed to describe these T_g dependencies, with the warmest T_g values found for high concentrations and fast cooling rates. These results emphasize the importance of considering T_g as a range rather than a discrete temperature. For all perchlorates measured, the degree of supercooling was extensive at high concentrations, exceeding 100 K from the liquidus. With a highly reduced glass temperature (T_g/liquidus temperature) and low critical rate of temperature change to avoid crystallization, concentrated perchlorate brines are strong glass formers when compared to other glass-forming materials. The consideration of cooling rates in the context of cellular cryopreservation suggests that cooling and warming rates may be an important astrobiological factors in a diverse set of planetary environments. These findings provide additional constraints on the possibility of liquid water on Mars in terms of concentration, different latitudes, seasons, and times of day.

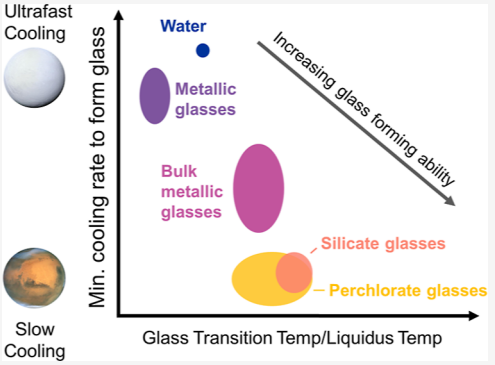

KEYWORDS: *perchlorates, glass transition, differential scanning calorimetry, brine, Mars, Europa, Enceladus, aqueous solutions*

INTRODUCTION

One of the major discoveries in the exploration of Mars has been the detection of perchlorate (ClO_4^-) in soils. First, the Phoenix lander detected perchlorate-containing soils in the arctic-equivalent region,[1] which generated considerable interest in the possibility for liquid brines on present-day Mars. Later, the Curiosity rover detected perchlorates in the equatorial region.[2] These results suggest that perchlorates are likely widespread on Mars, though in variable proportion relative to ubiquitous chlorides.[3]

Perchlorate salts may act as a potential repository of liquid water due to several properties. First, they are highly hygroscopic and adsorb or absorb water vapor even under extremely low water vapor concentrations; they also deliquesce into the aqueous phase.[4−6] Second, perchlorate brines can depress the freezing point of water and supercool below their eutectic temperature before crystallizing. The large supercooling of magnesium perchlorate ($Mg(ClO_4)_2$) and calcium perchlorate ($Ca(ClO_4)_2$) solutions has been proposed to potentially prevent water from freezing during diurnal and possibly annual cycles on Mars.[7] Recent work also suggests that current conditions on Mars may allow for stable brines on the surface and shallow subsurface at least for a small fraction of the year.[8,9] In addition to their application in planetary science, perchlorate solutions are essential to understanding the influence of ions on the physical behavior of a wide variety of aqueous processes since perchlorate holds the position of being one of the most chaotropic anions (disruptive of the hydrogen bonding network between water molecules) in the Hofmeister series.[10]

Glasses are disordered, non-crystalline materials that behave mechanically like solids. The most common route to this vitreous state is via supercooling where a viscous liquid is cooled fast enough to avoid crystallization. The glass transition on warming is the gradual and reversible transition from the relatively brittle glassy state into a viscous liquid. Such

Received: April 6, 2023
Revised: June 8, 2023
Accepted: June 28, 2023
Published: July 11, 2023

amorphous rigidity can be obtained by cooling a liquid fast enough to bypass crystallization;[11] the supercooling of a liquid allows for the retardation of nucleation and crystallization. The glass transition temperature (T_g) is the temperature of such a transition and can represent a range of values depending on the warming or cooling rates, pressure, concentration of the solution, and nucleation processes. The T_g has implications for the formation, dynamics, and potential habitability of perchlorate salt solutions.

Despite the importance of the glass transition and T_g, its value in perchlorate solutions has only been previously evaluated systematically for $Ca(ClO_4)_2$ in terms of concentration dependence in the range of −125 °C (2.9 *m*) to −112 °C (5.5 *m*) by Angell and Sare.[12] Gough et al.[4] also reported that $NaClO_4$ solutions remained liquid down to −50 °C, below the sodium perchlorate ($NaClO_4$) eutectic at −34.1 °C.[13] Evidence from large-vessel (~200 cm^3) cooling experiments by Toner et al.[7] suggest that $Mg(ClO_4)_2$ and $Ca(ClO_4)_2$ solutions do not crystallize during slow cooling rates of <1 K/min but remain in a supercooled liquid state until forming an amorphous glass estimated around 153 K.

In materials engineering, it is known that the values of T_g depend on both the warming rates and cooling rates of samples prior to measurements.[14,15] Such a dependence on thermal history has been noted for various glasses and amorphous materials, including arsenic triselenide, boron trioxide, potassium silicate, borosilicate crown glasses,[14] polymers,[16] lithium borosulfate glasses,[17] and potassium and calcium nitrates.[18] Glasses are also distinctive for exhibiting a glass transition upon cooling and/or warming.[19] The cooling and warming rate dependence of aqueous perchlorate solutions has not yet been investigated for any composition or concentration.

Salt solutions can be supercooled below temperatures where thermodynamic models predict crystallization of salt or ice. While a supercooled liquid is outside thermodynamic equilibrium, it can exist in a metastable, nonequilibrium state within local free energy minima. This metastable state may persist for very long times, even years.[20] Glasses are nonequilibrium materials.[21] The glass transition is a kinetic phenomenon with continuous changes in structure and properties between the liquid and solid (glassy) states.

There are two timescales relevant to glass formation: an internal timescale determined by the bonding and viscosity of the liquid and an external timescale controlled by the experimental cooling or warming rate of the liquid. A high initial viscosity of a liquid acts as a kinetic barrier to both nucleation and the rearrangement into the crystalline structure. The process of supercooling also requires the absence or minimization of nucleation sites since the presence of impurities, sample agitation, or even container contact may induce prompt crystallization.[19] Experimentally, it is found that T_g exhibits a dependence on the warming or cooling rate with higher values of T_g observed for faster warming or cooling rates.

The properties of a glass depend on this formation process. Slower cooling produces a lower T_g. The slower a liquid is cooled, the more dwell time at each temperature for the liquid to relax, and the colder it can become prior to falling out of the liquid-state equilibrium.[11] Since slower cooling allows the liquid to remain in equilibrium at lower temperatures, the glass solidifies at a lower temperature and the glass has properties corresponding to these lower temperatures. Accordingly, T_g decreases with slower cooling rates,[22] resulting in a denser and lower enthalpy glass than a glass that experienced faster cooling.[11] Conversely, at faster cooling rates, there is decreased time for the liquid to adjust to the temperature change (i.e., relaxation), resulting in a glass synthesized at a higher temperature that possesses the properties of that higher temperature, including a lower density and higher enthalpy.[19]

For pure water, preventing crystallization requires hyperquenching the liquid at extreme cooling rates on the order of 10^7 $K{\cdot}s^{-1}$[23] resulting in an ambient pressure T_g at 136 ± 2 K, although this value has been highly debated as its calorimetric signature is very feeble.[24] Once an amorphous glass, water can be heated up to approximately 150 K without nucleation.[21] Similarly, NaCl solutions do not vitrify at normal pressure under normal cooling procedures.[25] While pure water is not considered to have a high glass-forming ability, the addition of perchlorates may drastically alter its tendency toward glass formation.

Vitrification is a cryopreservation strategy potentially important for astrobiology that enables living cells to be cooled to cryogenic temperatures without the harmful crystallization of ice. As opposed to freezing, vitrification allows cells to survive very low temperatures.[26] Liquid water exists in a disordered state inside living organisms. During vitrification, it is advantageous to maintain the natural disorder of water molecules so the system being preserved is minimally disturbed.[26,27] In cryobiology, practical vitrification methods used for cryopreservation of cells include dilute solutions cooled at very quick rates and very concentrated solutions vitrified at very slow cooling rates.[27]

On Earth, freeze avoidance by supercooling and vitrification are survival mechanisms employed by polar species in extreme environments.[28] Unlike intracellular freezing, microbes can employ vitrification as a strategy to avoid death, allowing cells to survive very low temperatures.[27] Life forms on Mars or other icy worlds could utilize a similar survival mechanism, either by producing their own organic cryoprotectants[29] or in supercooled or glassy brine solutions. Vitrified brines may be important in the context of astrobiological targets for the future exploration missions "of icy worlds", such as Mars, Enceladus, Europa, Ganymede, Callisto, and Titan. Even concentrated perchlorate brines may host extremophile life, as significant perchlorate tolerances have been reported for Archaea, Bacteria, and Eukarya (Fungi) (ref 30 and references therein).

As cold, concentrated perchlorate salt solutions are not known to occur within natural environments on Earth, laboratory experiments are required to explore their properties. In this study, we determine the glass transition temperatures as a function of concentration and temperature ramp rate in aqueous $NaClO_4$, $Ca(ClO_4)_2$, and $Mg(ClO_4)_2$ solutions using differential scanning calorimetry (DSC). DSC is a thermal analysis technique that measures the heat flow into or out of a sample as a function of temperature or time, while the sample is subjected to a controlled temperature program. We examined the temperature effects from −140 to 25 °C, which essentially covers the temperature range observed for Mars' surface, from −123 to 27 °C.[31] To investigate the magnitude of supercooling in aqueous salt solutions and how vitrification is influenced by salt composition, concentration, and the cooling or warming rate, we monitored the heat flow of perchlorate brines during cooling and warming in DSC experiments.

https://doi.org/10.1021/acsearthspacechem.3c00090
ACS Earth Space Chem. 2023, 7, 1433−1445

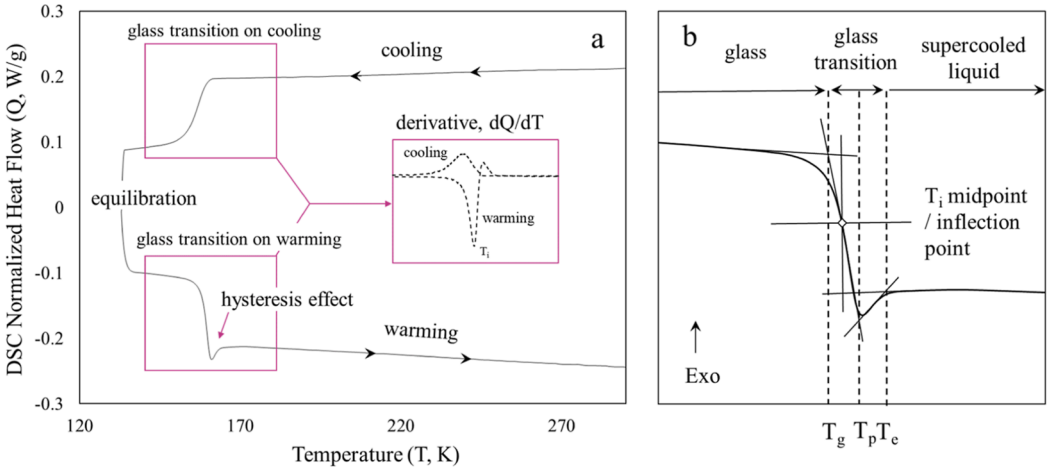

Figure 1. (a) Example of a DSC thermogram for the glass transition temperature for $Mg(ClO_4)_2$ with the derivative of the heat flow. (b) Schematic of the DSC warming curve of the glass transition, where T_g, T_p, and T_e are the onset temperature, the peak temperature, and the end temperature of the glass transition, respectively, while T_i indicates the midpoint or inflection point and is the minimum on the first derivative. The thermograms are shown with exothermic (exo) peaks up.

Table 1. Summary of DSC T_g Measurements for $Mg(ClO_4)_2$, $Ca(ClO_4)_2$, and $NaClO_4$

		$Mg(ClO_4)_2$		
ΔT (K/min)	4.3 mol/kg	3.9 mol/kg	3.5 mol/kg	3.0 mol/kg
150	161.7	159.8	157.7	155.6
75	160.3	158.1	155.9	154.2
50	159.4	157.2	155.1	153.3
20	157.4	155.4	153.4	151.3
10	156.1	154.0	152.0	150.0
5	154.9	153.0	151.1	148.8
		$Ca(ClO_4)_2$		
ΔT (K/min)	6.0 mol/kg	5.5 mol/kg	5.0 mol/kg	4.3 mol/kg
150	164.6	162.4	158.9	155
75	163.6	161.2	157.4	154
50	162.5	160.3	156.6	153.1
10	160.5	157.8	154.5	150.7
5	159.3	156.5	153.2	149.5
		$NaClO_4$		
ΔT (K/min)	16.0 mol/kg	13.3 mol/kg	12.3 mol/kg	11.5 mol/kg	11.0 mol/kg
150	173.5	168.7	166.3	165.2	163.9
100	172.9	167.8	165.5	164.7	163.2
75	172.1	167.2	164.7	164.2	162.3
50	171.4	166.6	164.1	163.2	161.5
20	169.6	164.5	162.7	161.2	160.2
10	168.4	163.2	161.5	160.0	158.9
5	167.2	162.1	160	158.9	157.7
1	164.4	159.1	157.7	156.2	155.1

METHODS

The T_g measurements were made using a Q2000 DSC manufactured by TA Instruments. The DSC was cooled with liquid nitrogen, and helium was used as a purge gas at a flow rate of 25 mL min^{-1}. Near-saturated stock solutions of $NaClO_4$, $Mg(ClO_4)_2$, and $Ca(ClO_4)_2$ were prepared using Sigma-Aldrich salts dissolved into 18 MΩ deionized water. Samples were prepared immediately before each DSC analysis to minimize hygroscopic contamination. For each sample, 20 μL (20−30 mg) of solution was pipetted into Tzero Alodine-coated aluminum sample pans, and then each pan was sealed hermetically with an aluminum lid to prevent vapor transfer or sample contamination. To ensure that the lid remained hermetically sealed over the course of the experiment, the weight of sample pan, lid, and aqueous sample was determined before and after the DSC analysis to an accuracy of ±0.001 mg. Empty pans and deionized water were also run as controls. The kinetic behavior of the glass transition region was observed by monitoring its dependence on the cooling and warming rate, specifically by investigating different rates from 1 to 150 K/min in the range of −140−25 °C. The ratio of cooling and warming rates influences the shape of the DSC curves.[15] Most accurate results are attained in experiments when an initial cooling rate is equal to a heating rate.[14,15] Therefore, samples used for model calibration were cooled and warmed at the same rate in this study.

https://doi.org/10.1021/acsearthspacechem.3c00090
ACS Earth Space Chem. 2023, 7, 1433−1445

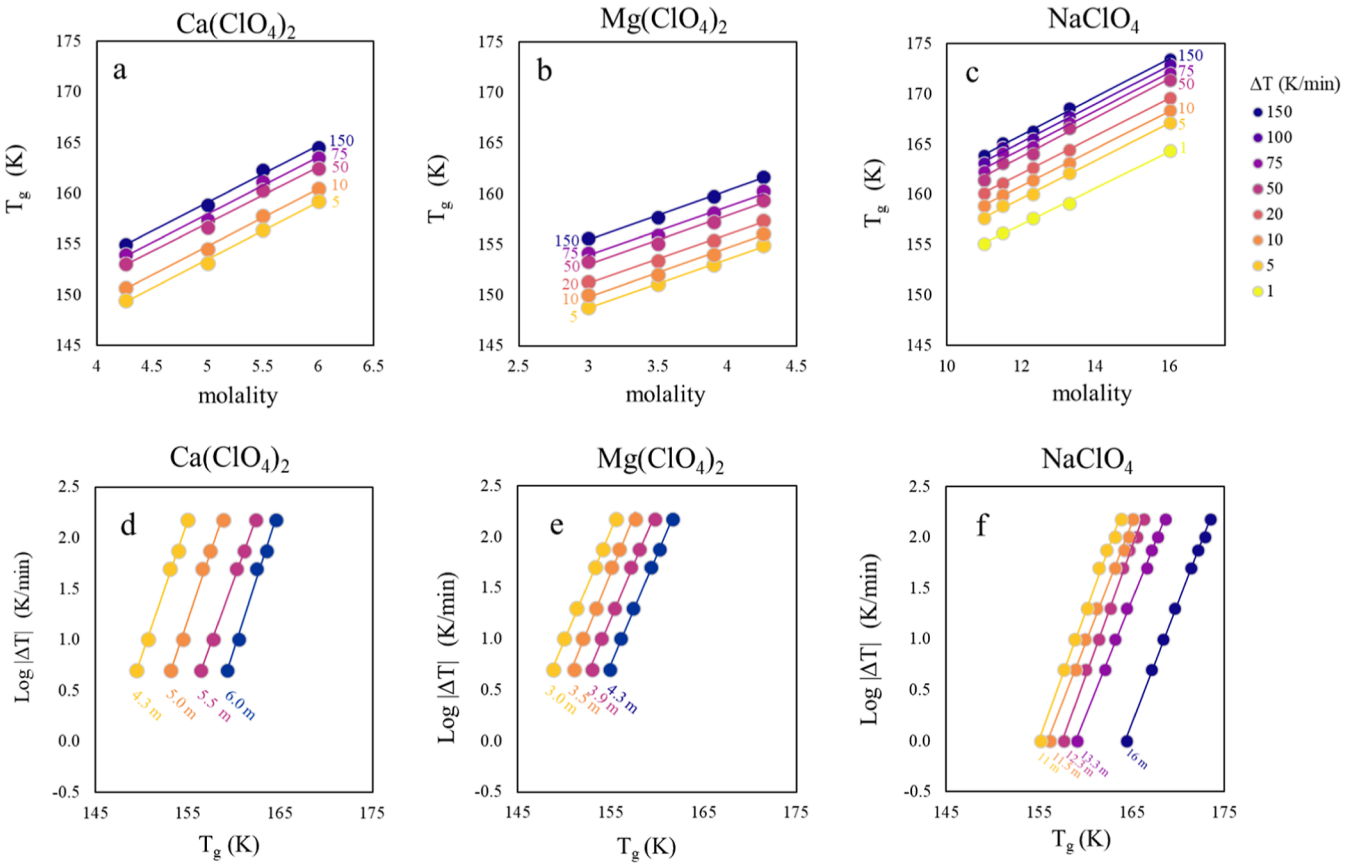

Figure 2. (a–c) Variation of the onset T_g versus concentration in molality (mol/kg) for $Ca(ClO_4)_2$, $Mg(ClO_4)_2$, and $NaClO_4$ solutions. (d–f) Variation of the onset T_g with the warming rate of the glass. The T_g depends on both the concentration of the perchlorate solution and the warming/cooling rates.

Figure 1 shows an example of a DSC thermogram for the glass transition temperature region with measured points denoted. The glass transition temperature (T_g) was recorded as the onset or end point extrapolated to the baseline using TA Instruments TRIOS software. Unlike the freezing point, the glass transition is not a true transition temperature since vitrification occurs over a temperature interval and is marked by several features (Figure 1). The T_g was confirmed by taking the first derivative of the DSC heat flow curve.

Thermal lag is proportional to heat flow, heating rate, and the mass of the sample/pan system. Thus, the thermal lag error increases with fast scanning rates, large sample masses, large sample pans, or samples with high heat capacities. For our experiments, all data have been corrected for the thermal lag caused by the sample pan and the DSC cell. Using the inbuilt independent sensor on the DSC disk (in addition to the sample and reference temperature sensors), it is possible to calibrate the thermal lag characteristics of both the cell and of the pan encapsulating the sample. The thermal resistance and capacitance of each pan type as a function of temperature is built into the TA software, thereby allowing thermal lags caused by the pan to be addressed within each sample program. As reported by the instrument manufacturer, virtually all scanning rate-dependent thermal lag is eliminated in the Q2000 DSC. Further, care was taken to run samples at a range of different rates (1– 150 K/min) to monitor for and minimize adverse rate-dependent effects. For example, thermal lag may compromise samples run at high-temperature ramp rates, while low signal-to-noise ratios may compromise samples run at low-temperature ramp rates.

RESULTS

The absence of spikes, troughs, or temperature plateaus in the DSC thermograms indicate that $Ca(ClO_4)_2$, $Mg(ClO_4)_2$, and $NaClO_4$ solutions remained liquid below their respective freezing points. Neither the crystallization of ice nor the precipitation of salt phases was observed. Therefore, a number of experiments demonstrated effective supercooling and glass formation. It has previously been estimated that for many materials, the T_g dependence on the cooling rate is relatively weak with an order of magnitude change in cooling rate only affecting a T_g shift of 3–5 K.[20] However, for organic compounds, a greater dependence on rate has been reported with an increase of 5–6 K as the cooling rate changes from 2 to 10 K/min for certain compounds.[32] Here, we found that the effect of the temperature rate was significant but not extreme for any of the perchlorates measured, ranging from 8 to 10 K between rates of 1 and 100 K/min. The 1 K/min rate refers to the warming rate only since the cooling rate often had to be greater than the warming rate to prevent crystallization; these multi-rate experiments were not used to calibrate the T_g parameterization model described below. Experimental results are listed in Table 1 and visualized in Figure 2.

Figure 3 compares the literature values of previous $Ca(ClO_4)_2$ glass transition measurements with our data. The inflection points of the glass transition on warming at 10 K/min for 5.0, 4.2, and 3.0 *m* $Ca(ClO_4)_2$ solutions were measured

https://doi.org/10.1021/acsearthspacechem.3c00090
ACS Earth Space Chem. 2023, 7, 1433–1445

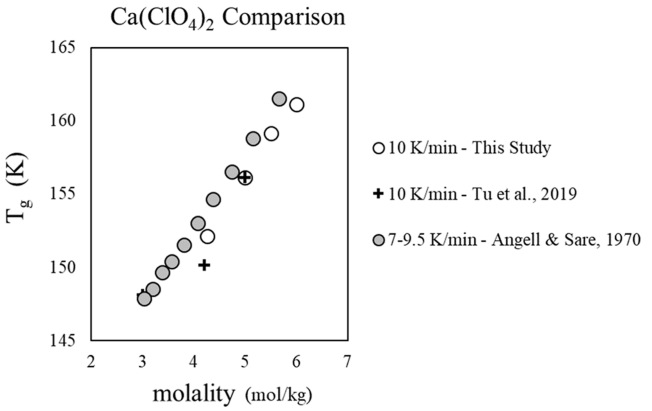

Figure 3. Literature comparison for previous T_g measurements for $Ca(ClO_4)_2$ solutions with concentration in molality (mol/kg). The results of this study and Tu et al.,[33] using DSC onset temperatures for the determination of T_g, are in good agreement.

with DSC curves by Tu et al.,[33] Angell and Sare[12] reported the T_g for varying concentrations of $Ca(ClO_4)_2$ solutions using a 4 mm diameter Pyrex glass tube with an inserted thermocouple and a warming rate of 7−9 K/min after rapid cooling. The data from Tu et al.[33] and Angell and Sare[12] fall within the expected bounds of this study given the differences in experimental setup and measurement. The concentration dependence is roughly consistent across all studies.

According to the data shown in Figure 2, the T_g in K can be parameterized in terms of concentration and temperature rate using the general form of the equation

$$T_g\ (\mathrm{K}) = a(\mathrm{molality\ (mol/kg)}) + (b \times \log \Delta T\ (\mathrm{K/min}) + c) \quad (1)$$

where a, b, and c are experimentally determined constants for each type of salt and are given in Table 2. The standard error for each parameter (±) is given in Table 2, which was calculated in Python with the SciPy library with the *curve_fit* function from the *scipy.optimize* module, where the function performs a nonlinear least-squares fit minimizing the sum of the squares of the residuals between the predicted values and the actual data. The *curve_fit* function returns two values: popt, which is an array of the optimal values for the parameters, and *pcov*, which is the estimated covariance matrix of the parameters. The diagonal elements of *pcov* provide the variance estimates for the parameters, and the square root of these values gives the standard errors. A comparison of the experimental data to the model is shown in Figure 4.

Table 2. Parameters for Eq 1[a]

	a	±	b	±	C	±
$Ca(ClO_4)_2$	5.63	0.050	4.11	0.202	122.24	1.564
$Mg(ClO_4)_2$	4.84	0.073	4.83	0.220	130.96	0.433
$NaClO_4$	1.90	0.054	3.91	0.174	134.27	0.453

[a]Here "±" indicates the standard error on each parameter.

The coefficient a represents the sensitivity of T_g to molality, where larger values of a indicate a stronger concentration dependence. The values of coefficient a of $Ca(ClO_4)_2$ (a = 5.63 ± 0.050) and $Mg(ClO_4)_2$ (a = 4.84 ± 0.073) have a similar dependence on the concentration, while for $NaClO_4$ (a = 1.90 ± 0.054) it is significantly lower, indicating a weaker dependence on the concentration. The brines may be ranked in terms of greatest to least concentration dependence as follows: $Ca(ClO_4)_2$, $Mg(ClO_4)_2$ > $NaClO_4$. This is consistent with the finding that for electrolyte solutions, especially those of multivalent cations, the value of T_g is greatly influenced by composition, and the required concentration for bulk vitrification depends on the cation charge.[25] The coefficient b represents the sensitivity of T_g to the logarithm of the rate of temperature change, ΔT, with larger values of b indicating a stronger dependence. Within the standard error for b, the salts have a similar sensitivity of T_g to the logarithm of ΔT.

For intermediate-strength glass-forming cryoprotectant solutions, such as glycerol and other polar liquids with hydrogen bonds, T_g has been reported to occur over a temperature interval of approximately 10 K.[27] We confirm a similar transformation interval for perchlorate brines. For $Mg(ClO_4)_2$, the end temperature (T_e) of the glass transition upon warming occurred approximately 6 K after the onset temperature (T_g), while for $Ca(ClO_4)_2$, the difference was approximately 5 K. $NaClO_4$ showed the largest glass transition range with approximately 7.5 K separation between T_g and T_e. Figure 5 shows the temperature interval for the glass transition region for different perchlorate brines at varying concentrations and warming rates. The modeled T_g and T_e are shown in Figure 6 using the above eq 1 and these offsets. A glass transition was noted both on cooling and on warming in all experiments. The T_g on cooling is only offset by approximately

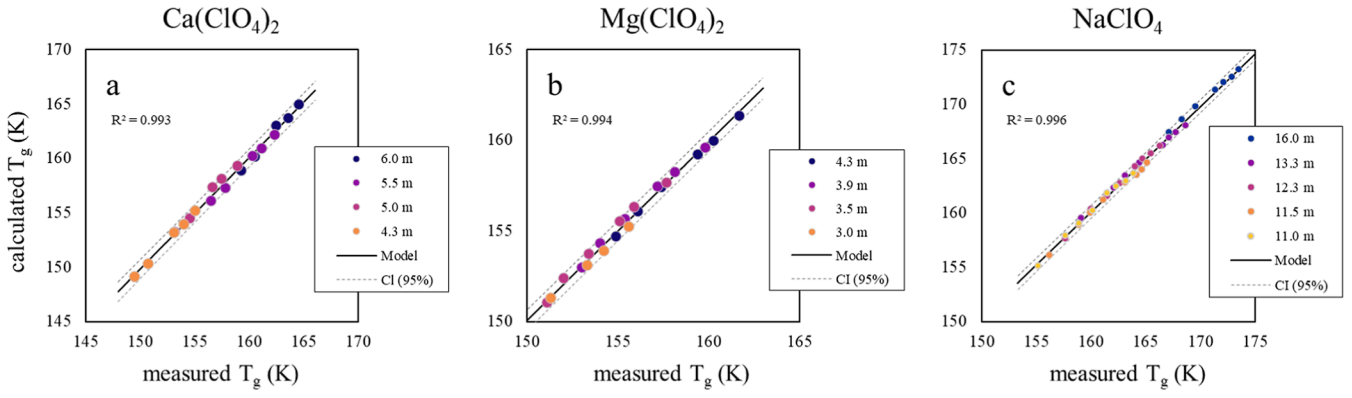

Figure 4. Comparison of experimental data to model from eq 1. All data fall on or within a 95% confidence interval and exhibit a high degree of linearity (R^2). For $NaClO_4$, data obtained at 1 K/min, which was not used to fit the parameters, is still in good agreement with the model.

https://doi.org/10.1021/acsearthspacechem.3c00090
ACS Earth Space Chem. 2023, 7, 1433−1445

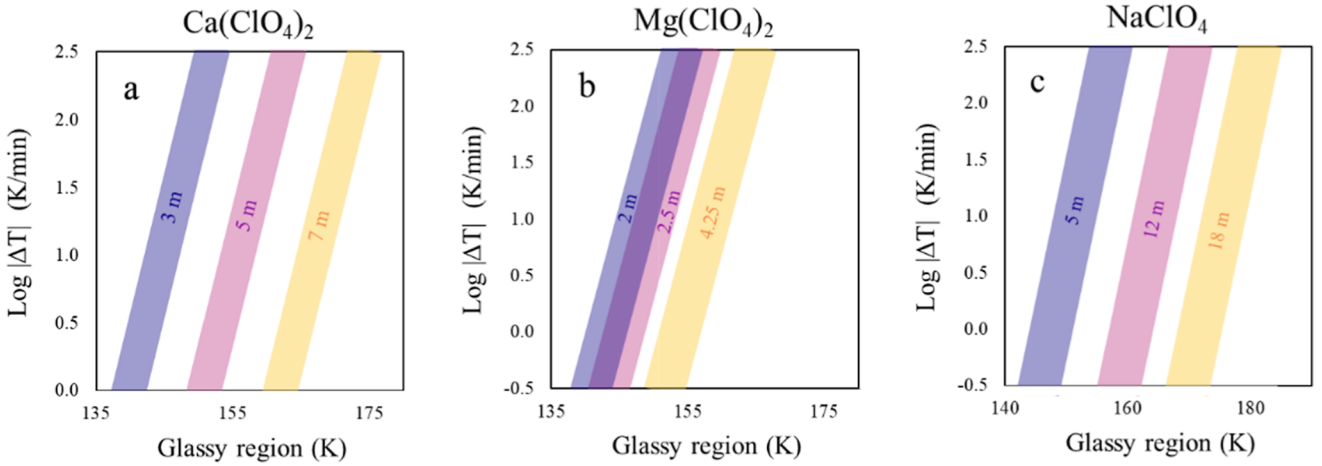

Figure 5. Temperature range for glassy regions between T_g and T_e for (a) $Ca(ClO_4)_2$, (b) $Mg(ClO_4)_2$, (c) $NaClO_4$ at several concentrations reported in molality (m).

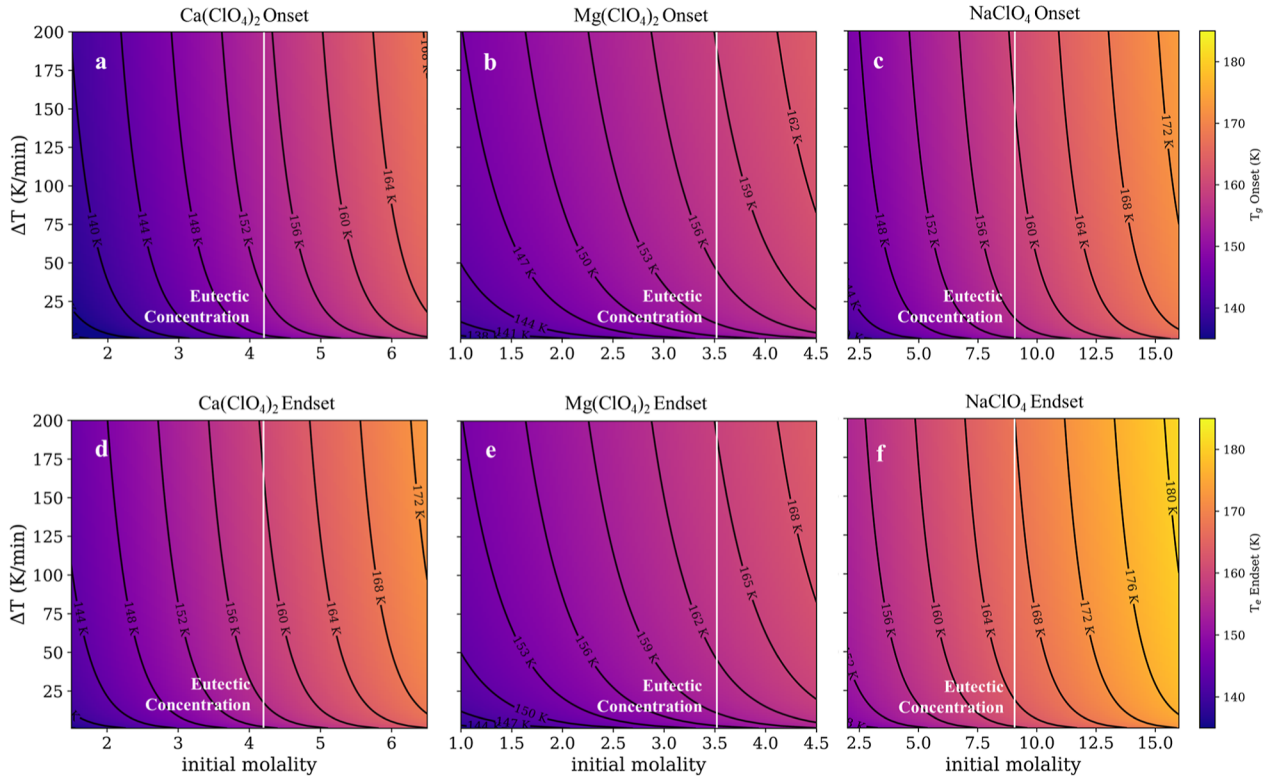

Figure 6. Data-constrained model of the effect of both concentration reported in molality (mol/kg) and warming rate on $Ca(ClO_4)_2$, $Mg(ClO_4)_2$, and $NaClO_4$ solutions, where (a–c) show the onset temperature (T_g) where the glass transition region begins, while (d–f) shows the end temperature of the glass transition, (T_e). The solid white line shows the eutectic concentration according to Toner et al.[34] Solid black lines show isotherms for T_g (a–c) or T_e (d–f).

2–3 K compared to on warming for all perchlorates studied, suggesting that hysteresis has only a small effect.

The results of this study demonstrate that the degree of supercooling until vitrification varies based on the salt composition, concentration, and the rate of formation. The degree of supercooling can be estimated by the temperature difference between T_g and the equilibrium temperature when ice or salt should have first crystallized. At the eutectic concentration, $NaClO_4$ can be supercooled by ~88 K from the liquidus, while the degree of supercooling is ~127 K at concentrations near saturation (Figure 7). Similarly, the degree of supercooling below the eutectic for $Ca(ClO_4)_2$ is ~55 K, while it is ~131 K at concentrations near saturation. At the eutectic concentration, $Mg(ClO_4)_2$ can be supercooled by ~56 K from the liquidus, and near saturation the degree of supercooling is ~156 K. This is a large degree of supercooling, considering that Queiroz and Šesták[19] estimated that supercooling is often only 10–20 K below the liquidus for many glass-forming materials.

In general, supercooling of the bulk solution is more easily achieved in concentrated solutions, assuming no salt precipitation. Below the eutectic concentration, crystallization of water ice may enable perchlorate supercooling. As H_2O ice crystallizes, the dissolved salt in the remaining liquid will

https://doi.org/10.1021/acsearthspacechem.3c00090
ACS Earth Space Chem. 2023, 7, 1433–1445

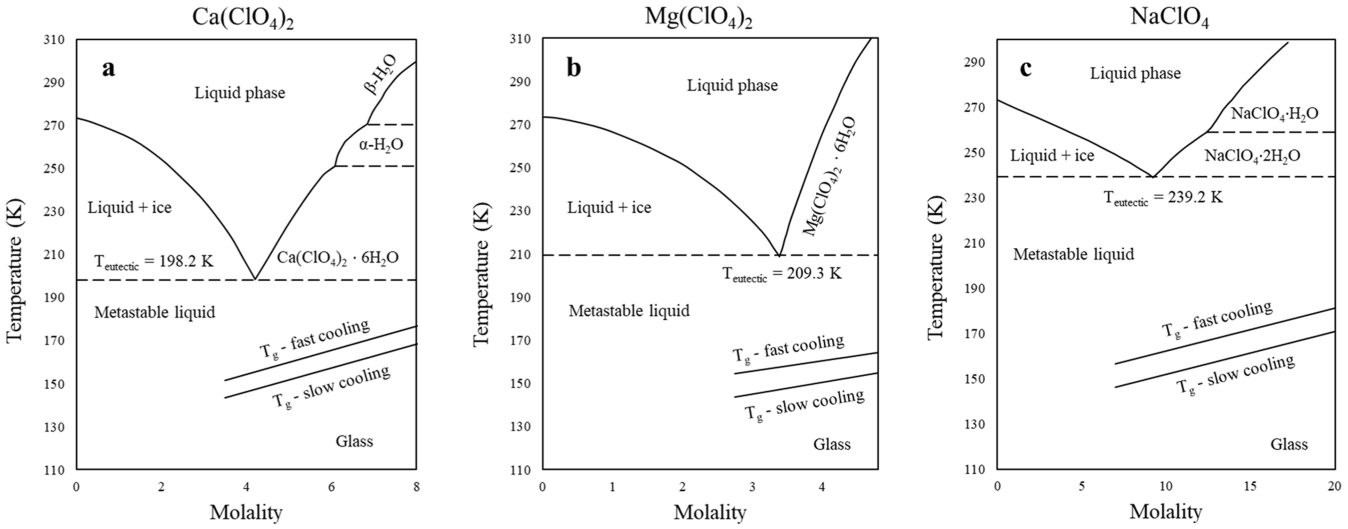

Figure 7. Phase diagrams for (a) $Ca(ClO_4)_2$, (b) $Mg(ClO_4)_2$, and (c), $NaClO_4$ from solubility data from Toner et al.[34] with T_g curves added. Solid lines indicate ice solubilities and salt solubilities, with the dotted line showing the eutectic temperature. Below the eutectic, the glass phases (calculated as T_g onset) formed via supercooling are shown for both fast (200 K/min) and slow rates (0.5 K/min). A viscous liquid phase may also form if a glass is not synthesized.

become concentrated. Therefore, while it is more difficult to synthesize pure glass absent of crystallization events, dilute solutions of perchlorate brines may still produce supercooled liquids or glasses in a mixed phase system consisting of H_2O ice crystals and viscous brines or glasses. Such a situation was noted in a number of dilute experiments that failed to synthesize pure glass. For example, for a 1 *m* $Mg(ClO_4)_2$ experiment, there was clear evidence of both water ice crystallization upon cooling and glass transition features, where the measured T_g was consistent with a concentration of ∼4 *m*. This suggests that ∼25% of the original liquid mass was residual after crystallization. In such a scenario, it may still be possible for microorganisms to enjoy the preservation benefits of glass formation by occlusion from the ice crystals in order to be preserved in the liquid/glass phase.

DISCUSSION

Glass-Forming Ability. The contest between vitrification and nucleation occurs not only in perchlorate brines but also in various classes of materials with various types of bonding. Perchlorate glasses can be placed into the context of other glass-forming materials by considering whether they are weak or strong glass formers. A strong glass former has a low critical rate, which is the cooling or warming rate needed to avoid crystal formation.[25] If prepared above a critical concentration, the majority of aqueous solutions of multivalent cation salts, and of many lithium salts, can be considered good glass formers.[25] The critical cooling and warming rates of a glass depend on a number of parameters, including the glass-transition temperature, liquidus temperature, thermal diffusivity, sample thickness, pressure, quench structures, and sample confinement. Therefore, depending on experimental conditions, glasses of the same composition may have different critical rates.[35]

When compared to other glass-forming liquids, from poor (water) to excellent (silicate glasses), post-eutectic perchlorate brines exhibit exceptional glass-forming ability with a remarkably low critical rate, even assuming a range from 0.2 to 5 K/min. The suppression of crystallization by supercooling remains one of the best indicators of a liquid's glass-forming ability.[36]

According to our results, the critical concentration for perchlorate brines to avoid ice crystallization is at or near to the eutectic temperature. A further upper limit on critical concentration may also be considered where the brine must be dilute enough to avoid hydrate precipitation. During X-ray scattering experiments, Tu et al.,[33] noted that a cooling rate of 6 K/min caused 3.5 and 5.0 *m* $Ca(ClO_4)_2$ solutions to crystallize before reaching −80 °C, with only the intermediate 4.2 *m* sample of $Ca(ClO_4)_2$ supercooling to −100 °C without crystallization of either ice or hydrate. Toner et al.[7] noted four distinct precipitation/dissolution events in a 7 *m* $Ca(ClO_4)_2$ solution cooled at <1 K/min, where bulk vitrification was only possible at 4 *m* $Ca(ClO_4)_2$ and 3.4 and 4.2 *m* $Mg(ClO_4)_2$. When bulk vitrification was attempted in this study at a 1 K/min rate on a 4 *m* $Ca(ClO_4)_2$, three distinct exothermic peaks were visible, indicating unsuccessful bulk vitrification. This difference in reported critical cooling rates between Tu et al.,[33] Toner et al.,[7] and this study may be attributed to experimental and analytical differences. A smaller-volume setup as used by Tu et al.[33] and this study should advantage glass formation over larger-volume experiments. It is likely that these exothermic events could not be detected in the less sensitive setup of Toner et al.[7]

The reduced glass transition temperature (T_{rg}) is given by the ratio of the glass transition temperature to the liquidus temperature (T_m)

$$T_{rg} = \frac{T_g}{T_m} \tag{2}$$

The T_{rg} can be considered a criterion for ascertaining the suppression of crystallization in supercooled melts and hence the glass-forming ability of the liquid. A liquid with $T_{rg} = 2/3$ is very slow in crystallization on the laboratory timescale and only crystallizes within a very narrow temperature range.[36,37] Such a liquid is highly susceptible to supercooling into a glass state at slow rates. This ratio, referred to as the Turnbull criterion remains an excellent "rule of thumb" for predicting

https://doi.org/10.1021/acsearthspacechem.3c00090
ACS Earth Space Chem. 2023, 7, 1433−1445

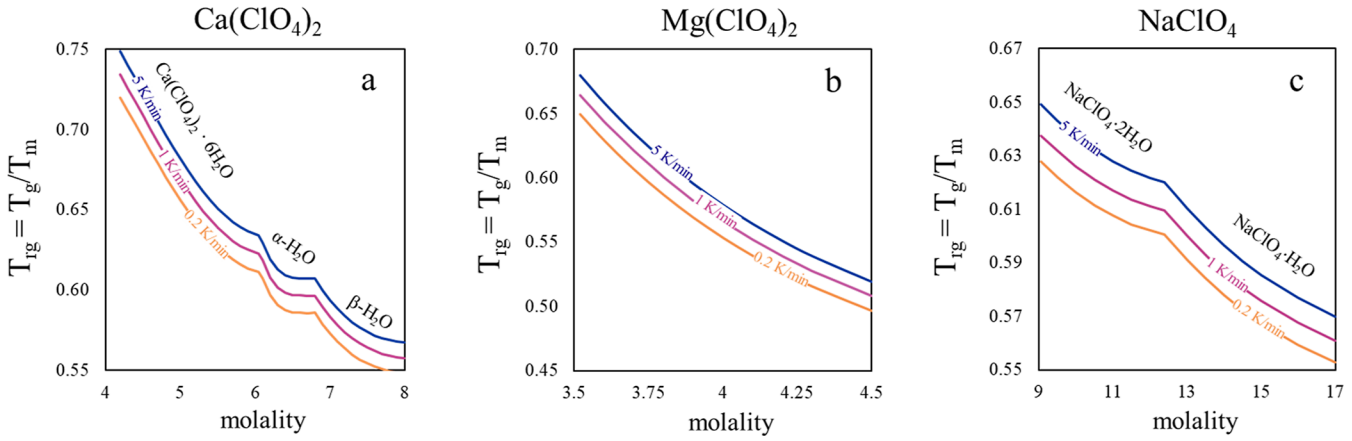

Figure 8. Reduced temperatures for Ca, Mg, and Na perchlorate brines. Kinks in the T_{rg} curves are caused by transitions between polymorphs or changes in the hydration state in the liquidus. Polymorphs for Ca are indicated where a phase transition occurs at 253.6 K due to the dehydration of $Ca(ClO_4)_2{\cdot}6H_2O$ to α-$Ca(ClO_4)_2{\cdot}4H_2O$ and a phase transition at 270.8 K due to the formation of β-$Ca(ClO_4)_2{\cdot}4H_2O$.

the glass-forming ability of any liquid[37] and allows for the comparison of different types of glasses. The range of T_{rg} values for different critical rates (0.2, 1, 5 K/min) are given in Figure 8 for various concentrations of each perchlorate and the range reported in Table 3. The mean T_{rg} at the eutectic

Table 3. Reduced Temperature (T_{rg}) for Perchlorate Brines

	T_{rg} min	T_{rg} max	mean T_{rg} at eutectic
$Ca(ClO_4)_2$	0.55	0.75	0.73 ± 0.01
$Mg(ClO_4)_2$	0.50	0.68	0.66 ± 0.01
$NaClO_4$	0.55	0.65	0.64 ± 0.01

concentration for each salt is shown for the different calculated critical rates. Figure 9 compares the critical rate versus the reduced glass transition temperature for different types of glasses.

The degree of supercooling below the eutectic for perchlorate brines strongly correlates with the eutectic temperature (Figure 10). The eutectic temperature also strongly correlates with the relative humidity at which deliquescence occurs (DRH) for electrolytes at 25 °C, which Tu et al.[33] interpreted as an ion pairing mechanism that also explains the propensity of perchlorates to prevent ice nucleation and easily deliquesce. Tu et al.[33] reported that for the supercooled regime, the number of solvent-shared ion pairs increased with decreasing temperature and that this heightened presence of solvent-shared ion pairs limited the formation of long-range order in the tetrahedral networks of water molecules, accounting for the extremely low eutectic point and deep supercooling of the $Ca(ClO_4)_2$ brines. While ionic strength under ambient conditions gives a first-order approximation for ion pairing, future work should continue to explore ion pairing and solvation effects in different salt compositions, especially with temperature variations.

Application to Mars and Icy Worlds. The supercooling and vitrification results of this study elucidate the potential for liquid brines to persist below their eutectic temperature on Mars. Here, we consider the supercooling below the eutectic temperature for each perchlorate studied and the range of plausible T_g values given a concentrated brine and a cooling rate relevant to Mars at the Phoenix landing site, where perchlorate has been detected at concentrations between 0.5 and 1%.[1] During Sol 19 of the Phoenix mission, the robotic

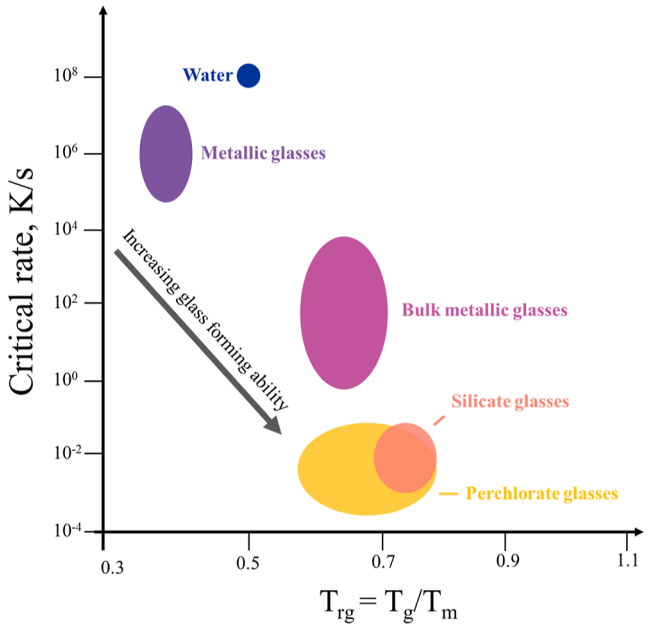

Figure 9. Critical rate versus reduced glass transition temperature $T_{rg} = T_g/T_m$, where T_g is the glass transition temperature and T_m is the liquidus or melting temperature (figure updated and modified from Ojovan[38]). Perchlorate data is from Table 3 and Figure 8.

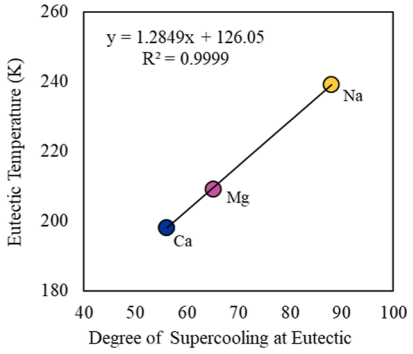

Figure 10. Correlation between the eutectic temperature and the degree of supercooling, where the degree of supercooling refers to the amount of supercooling below the eutectic temperature.

https://doi.org/10.1021/acsearthspacechem.3c00090
ACS Earth Space Chem. 2023, 7, 1433−1445

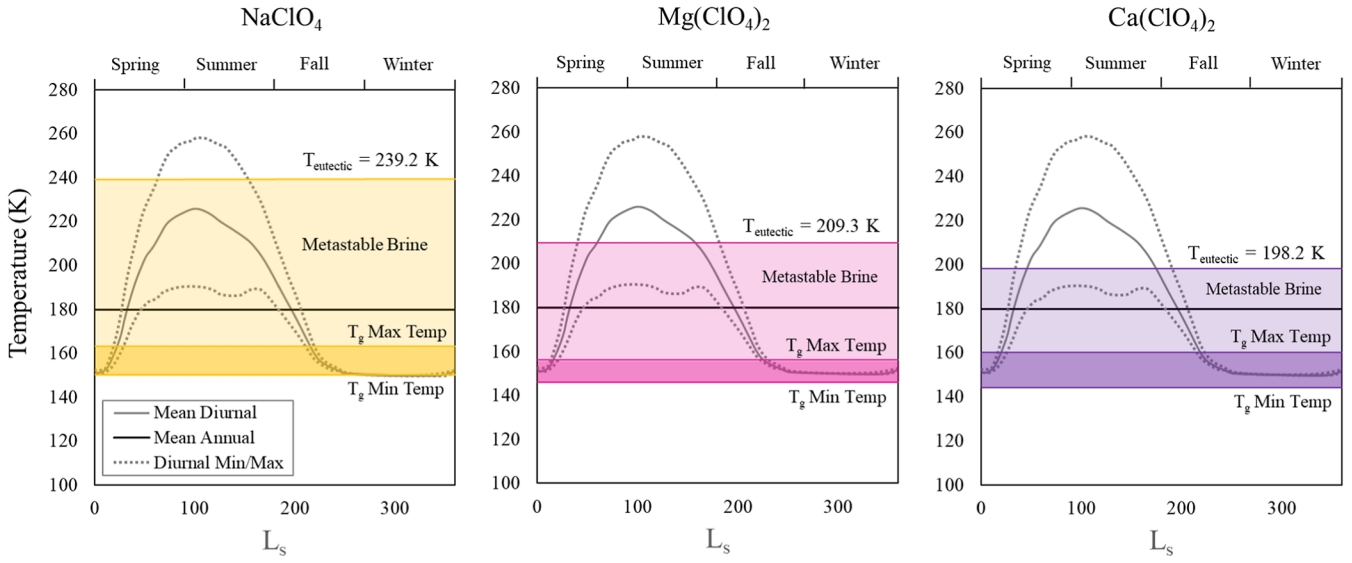

Figure 11. Degree of supercooling from the eutectic temperature until vitrification for (a) $NaClO_4$, (b) $Mg(ClO_4)_2$, and (c) $Ca(ClO_4)_2$ illustrated at the Phoenix site (68.22°N, 234.25°E). A range of plausible vitrification temperatures are depicted in the darker region, where T_g Min Temp denotes the T_g for the eutectic concentration, while T_g Max Temp denotes a brine near saturation. The lighter shaded region shows where a supercooled brine is permitted. The mean annual, mean diurnal, and diurnal maximum/minimum temperatures are from ref 7 and were originally generated using the Mars Climate Database.[46]

arm excavated ice from a depth of ∼5 cm with little resistance.[39] This finding led to the suggestion that the "soft ice" was likely frozen brine, which is known to be softer than freshwater ice.[40,41]

To determine the diurnal cooling rate ($|\Delta T|$ (K/min)) applicable to the Phoenix site for the utilization of eq 1, multiple estimates were taken into consideration. Phoenix's thermal and electrical conductivity probe (TECP) measured the ground temperature during 16 sols, with sporadic diurnal reporting on each of these sols.[42] Using the complete set of TECP soil temperature measurements, we calculate the diurnal cooling rate as ∼0.2 K/min.[42] The daytime maximum temperature of ∼259 K was achieved on sol 71 at L_s ∼ 107°, while the nighttime minimum values were as low as ∼180 K at L_s ∼ 133° on sol 122, which was the last sol with nighttime measurements.[43] However, the coupling of the TECP needles with the regolith was insufficient, and "direct and accurate regolith temperature measurement with TECP, as implemented on Phoenix, is not possible".[42] Instead, numerical models of the regolith are preferred to accurately calculate ground temperatures.[42,44] Based on numerical simulations of the ground temperature at the Phoenix landing site on sol 19,[44] the cooling rate of the ground is ∼0.3 K/min. The temperatures on sol 19 were notably colder than when the first ground temperature measurement by the TECP occurred on sol 46.[44] The nature of the surface material can also increase or decrease the surface temperatures and cooling rate. Low thermal inertia material, such as a fine-grained regolith, will cool far faster through the night and warm to a greater degree during the day than a high thermal inertia material, such as a homogenous rocky surface.[45] The estimated cooling rates for the Phoenix site fall between the thermal inertia models for a fine regolith or dust (∼0.7 K/min) or exposed rock (∼0.1 K/min).[45] Using a rate of 0.3 K/min, the cold temperatures required for vitrification of perchlorate brines are reachable in the Martian winter, while the metastable liquid above the T_g remains well within the feasible Martian temperature range over multiple seasons (Figure 11).

If seasonal glasses are formed on Mars, they could enjoy stability under long timescales, given appropriate temperature constraints. The observed supercooling indicates the potential stability for liquid water as a perchlorate brine during the spring and summer at a high latitude location on Mars, while during the winter, the supercooled brine may transition and persist in a glassy state. Further, experiments at 77 K on hyperquenched glassy water demonstrate high kinetic stability, where the glass can be stored for many years at ambient pressure.[47] Diurnal subsurface model simulations for a depth of 3 cm at the Phoenix landing site suggest warmer temperatures and higher relative humidity conditions compared to the surface,[6] where the temperature range of ∼240−215 K would be conducive to the formation of a stable brine above the eutectic for the divalent perchlorates or a metastable brine for $NaClO_4$.

While this study focused on single salt solutions, brines on Mars and other icy worlds will more realistically contain a mixture of salts, which may even increase the potential for vitrification. The perchlorate-H_2O system presented here probably represents a conservative constraint on supercooling and glass formation for perchlorate brines. In a mixed salt system, where the pure water component of our experiments is replaced with a different brine composition, the solution viscosity may increase to a certain concentration threshold without the disruption of the perchlorate glass network. This enhanced viscosity will kinetically inhibit crystal nucleation. Indeed, the glass transition can be described through the lens of viscosity. Regardless of the initial viscosity or nature of the liquid undergoing vitrification, the viscosity experiences a staggering increase near the T_g, approaching a value 10^{15} times higher than that of pure water.[12,27] The inclusion of chlorate, chloride, nitrate, or sulfate is expected to result in a significant increase in viscosity of the perchlorate brine, thereby further increasing the potential for the existence of supercooled brines and vitrification.

In future studies, the empirical parameterization approach described in this work could be applied to brine systems on icy

https://doi.org/10.1021/acsearthspacechem.3c00090
ACS Earth Space Chem. 2023, 7, 1433−1445

planetary bodies where cooling rate and concentration are important. Brine crystallization and vitrification kinetics are a necessary consideration considering the cooling rate in planetary contexts covers an expansive range from <1 K/min diurnally on Mars to ~10^4 K/s for plumes on Enceladus.[48] While NaCl solutions have received relatively more attention compared to other salts (e.g., refs 49 and 50), the critical concentration and critical cooling rates for many salts applicable to planetary brines remains unknown despite promising early results. For example, Raman data from Kanno and Hiraishi[51] suggested that aqueous solutions of magnesium salts with various anions (specifically $Mg(ClO_4)_2$, $MgCl_2$, $Mg(NO_3)_2$, and $MgSO_4$) formed glasses with cooling rates of 300−600 K/min with a concentration of 16 moles of water/moles of salt.

Data suggest that glasses exist on icy moons. Recently, Raman results on $MgSO_4$ hydrate indicate that the vitreous form likely exists on Europa.[52] Observations indicate that Europa has primarily amorphous ice, Ganymede contains both amorphous and crystalline ice, Callisto is mostly crystalline,[53] while Enceladus has both crystalline and amorphous ice.[54] The occurrence of such glassy material may be the result of multiple mechanisms, including propensity for glass formation from salts, the quick cooling rates resultant from cryovolcanism, or irradiation by high-energy particles.[53] Therefore, vitrification and metastability may be a widespread phenomenon on icy worlds.

Importance of Cooling Rate to Cryopreservation. The cooling rate has been identified as a key factor in determining the probability of survival during the cryopreservation of cells. Cell destruction generally occurs at either low (on the order of a few K/min) or high cooling rates (on the order of hundreds to thousands of K/min), with higher probabilities of cell survival falling between these extremes (ref 55 and references therein). In cryopreservation studies, the influence of cooling rate on survival can be described by the "Two-Factor Hypothesis" of freezing injury, which refers to the damage resulting from the opposing factors inherent to different cooling rates.[55] Three patterns emerge because of cooling rate effects on cryopreservation: extracellular freezing, intracellular freezing, vitrification.[55,56] At slow cooling rates, solutions are prone to forming extracellular ice crystals that disrupt the osmotic balance between the intra and extracellular fluids causing osmotic drying of the cell and leading to cell death. At high cooling rates, sharp intracellular ice crystals are formed within cells, and this mechanical effect often leads to cell membrane leakage, compromising cell integrity. However, if intracellular ice formation can be bypassed, vitrification occurs increasing the chance of cell survival.[56] These three competing factors are illustrated in Figure 12.

While vitrification may improve viability at higher cooling rates, experimentally producing these rates for cryopreservation purposes is practically restricted. The common method of cooling by direct immersion in the cryogenic fluid, such as liquid nitrogen, results in drastic film boiling around the sample, covering the sample in vapor and preventing efficient heat transfer from the fluid to the sample.[56] Cryopreservation studies on two-factor cooling rates suggest that cell survival for various cell types falls between 0.1 and 10,000 K/min (e.g., ref 55 and references therein). Therefore, the optimal cooling rate depends on the cell type, and the optimal cooling rate can widely vary for different cell types.

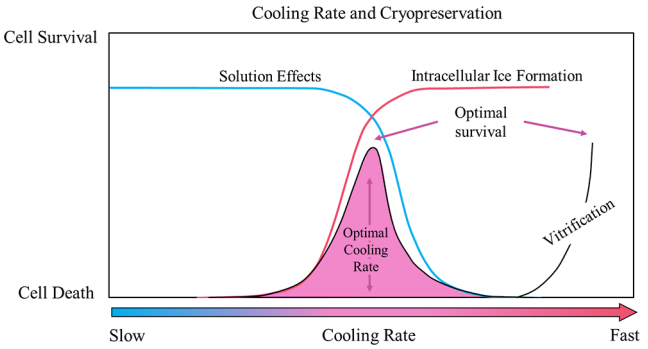

Figure 12. Simplified schematic showing the influence of cooling rate on cell survival as adapted from refs 55 and 56. At slow cooling rates, solution effects dominate, while fast cooling rates increase intracellular ice formation. At very fast cooling rates, vitrification preserves cells. Cell survival is maximized by minimizing these opposing factors at an optimal cooling rate that varies by cell and cryoprotectant type.

The cooling rates conducive to cell survival observed in cryopreservation studies fall within the range of cooling rates expected for aqueous and organic liquids in planetary contexts. Figure 13 shows a variety of different cooling rates in planetary

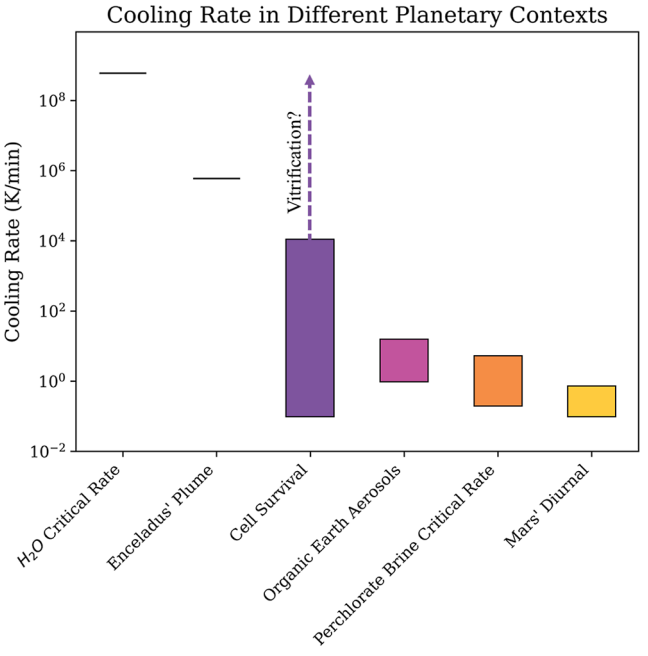

Figure 13. Comparison of the range of cooling rates (K/min) for various planetary environments and reference materials (listed on the *x*-axis). The upper and lower bounds of the boxes represent the maximum and minimum values, respectively, of the cooling rate in a planetary context or the critical rate of a reference material. The critical rate for water (needed to avoid crystallization and shown at the left) is given as an estimated upper limit on the expected critical rates for aqueous brines, given a very dilute brine will approximate the critical rate of water. The critical rate of perchlorate brines encompasses the slow diurnal cooling rates of Mars. Data is from the critical rate for water,[24] Enceladus' plume,[48] the range of cell survival[55] from 0.1 to 10,000 K/min, and organic aerosols on Earth[32] from 1 to 14 K/min. The data for perchlorate brines is from this study, while the Martian diurnal rate for the ground temperature is shown from 0.1 to 0.7 K/min.[45] Cooling and warming rates may be an important consideration for habitability and preservation in diverse planetary environments.

https://doi.org/10.1021/acsearthspacechem.3c00090
ACS Earth Space Chem. 2023, 7, 1433−1445

contexts as well as the critical rate for water and the critical rates determined for perchlorate brines. The critical rate for water is given as upper estimate on the expected critical rates for aqueous brines, since a very dilute brine can be approximated as water. On Earth, the glass transition of organic aerosols occurs for cooling rates in the range of 1−14 K/min and has important implications for aerosol reactivity, nucleation and growth, and cloud formation properties.[32] Supercooling and glass transitions in small, organic particles are likely to be relevant to Titan's haze, of interest for physical chemistry rather than cellular survival. The main haze is estimated to largely consist of 0.2 μm particles and surface temperatures are ∼94 K, decreasing to ∼71 K at the tropopause, and rise quickly to 160−180 K above the tropopause (ref 57 and references therein). The optimal cooling rate for cell survival encompasses the diurnal cooling rates found on Mars (Figure 13). While the quick cooling rates of Enceladus' plumes fall outside the optimal two-factor range, they may exist within the vitrification range. Therefore, cooling rates required for supercooling and vitrification do not necessarily preclude cell survival in a wide range of planetary environments.

CONCLUSIONS

We have systematically measured the supercooling and glass transition temperature (T_g) properties of concentrated Na, Ca, and Mg perchlorate brines using DSC in a temperature range applicable to Mars (−140 to 25 °C). Concentrations ranged from below the eutectic concentration to near saturation. We obtained the dependence of the T_g on the concentration and warming or cooling rate ranging from 1 to 150 K/min. The concentration and rate dependence can be described by a new, simple parameterization model, such that T_g (K) = a (molality (mol/kg)) + (b × log ΔT (K/min) + c), where a, b, and c are experimentally determined coefficients for each composition. Higher concentrations and faster rates of cooling produce a higher T_g temperature, whereas lower concentrations and slower rates of cooling produce a lower T_g. These differences may be significant, producing glass transitions with over 40 K difference. These results highlight that the T_g is not a discrete temperature but rather an environmentally dependent temperature range. A large amount of supercooling is possible prior to glass formation in concentrated perchlorates, with supercooling of up to 100 K below the liquidus. In the context of other glass-forming materials, concentrated perchlorate brines are strong glass formers, comparable to silicate glasses. An example application of the model reveals that the cold temperatures required for synthesizing glass from perchlorate brines are possible in the Martian winter, while the metastable liquid above the glass transition temperature may occur over multiple seasons. The results of this study allows for further constraints to be placed on the prospect of liquid water on present-day Mars in terms of concentration and the existence of brines at different latitudes, seasons, and times of day.

AUTHOR INFORMATION

Corresponding Author

Ardith D. Bravenec − *Earth and Space Sciences, University of Washington, Seattle, Washington 98195, United States;* orcid.org/0000-0001-9835-5173; Email: abravene@uw.edu

Author

David C. Catling − *Earth and Space Sciences, University of Washington, Seattle, Washington 98195, United States;* orcid.org/0000-0001-5646-120X

Complete contact information is available at: https://pubs.acs.org/10.1021/acsearthspacechem.3c00090

Notes

The authors declare no competing financial interest.

ACKNOWLEDGMENTS

We acknowledge support from the NASA Solar Systems Workings Program grant 80NSSC21K0149 and the NASA Habitable Worlds grant 80NSSC19K0311.

REFERENCES

(1) Hecht, M. H.; Kounaves, S. P.; Quinn, R. C.; West, S. J.; Young, S. M. M.; Ming, D. W.; Catling, D. C.; Clark, B. C.; Boynton, W. V.; Hoffman, J.; DeFlores, L. P.; Gospodinova, K.; Kapit, J.; Smith, P. H. Detection of Perchlorate and the Soluble Chemistry of Martian Soil at the Phoenix Lander Site. *Science* **2009**, *325*, 64−67.

(2) Ming, D. W.; Archer, P. D.; Glavin, D. P.; Eigenbrode, J. L.; Franz, H. B.; Sutter, B.; Brunner, A. E.; Stern, J. C.; Freissinet, C.; McAdam, A. C.; Mahaffy, P. R.; Cabane, M.; Coll, P.; Campbell, J. L.; Atreya, S. K.; Niles, P. B.; Bell, J. F.; Bish, D. L.; Brinckerhoff, W. B.; Buch, A.; et al. Volatile and Organic Compositions of Sedimentary Rocks in Yellowknife Bay, Gale Crater, Mars. *Science* **2014**, *343*, 1245267.

(3) Clark, B. C.; Kounaves, S. P. Evidence for the Distribution of Perchlorates on Mars. *Int. J. Astrobiol.* **2016**, *15*, 311−318.

(4) Gough, R. V.; Chevrier, V. F.; Baustian, K. J.; Wise, M. E.; Tolbert, M. A. Laboratory Studies of Perchlorate Phase Transitions: Support for Metastable Aqueous Perchlorate Solutions on Mars. *Earth Planet. Sci. Lett.* **2011**, *312*, 371−377.

(5) Gough, R. V.; Chevrier, V. F.; Tolbert, M. A. Formation of Aqueous Solutions on Mars via Deliquescence of Chloride−Perchlorate Binary Mixtures. *Earth Planet. Sci. Lett.* **2014**, *393*, 73−82.

(6) Nuding, D. L.; Rivera-Valentin, E. G.; Davis, R. D.; Gough, R. V.; Chevrier, V. F.; Tolbert, M. A. Deliquescence and Efflorescence of Calcium Perchlorate: An Investigation of Stable Aqueous Solutions Relevant to Mars. *Icarus* **2014**, *243*, 420−428.

(7) Toner, J. D.; Catling, D. C.; Light, B. The Formation of Supercooled Brines, Viscous Liquids, and Low-Temperature Perchlorate Glasses in Aqueous Solutions Relevant to Mars. *Icarus* **2014**, *233*, 36−47.

(8) Chevrier, V. F.; Rivera-Valentín, E. G.; Soto, A.; Altheide, T. S. Global Temporal and Geographic Stability of Brines on Present-Day Mars. *Planet. Sci. J.* **2020**, *1*, 64.

(9) Rivera-Valentín, E. G.; Chevrier, V. F.; Soto, A.; Martínez, G. Distribution and Habitability of (Meta)Stable Brines on Present-Day Mars. *Nat. Astron.* **2020**, *4*, 756−761.

(10) Zhang, Y.; Cremer, P. Interactions between Macromolecules and Ions: The Hofmeister Series. *Curr. Opin. Chem. Biol.* **2006**, *10*, 658−663.

(11) Debenedetti, P. G.; Stillinger, F. H. Supercooled Liquids and the Glass Transition. *Nature* **2001**, *410*, 259−267.

(12) Angell, C. A.; Sare, E. J. Glass-Forming Composition Regions and Glass Transition Temperatures for Aqueous Electrolyte Solutions. *J. Chem. Phys.* **1970**, *52*, 1058−1068.

(13) Hennings, E.; Heinz, J.; Schmidt, H.; Voigt, W. Freezing and Hydrate Formation in Aqueous Sodium Perchlorate Solutions. *Z. Anorg. Allg. Chem.* **2013**, *639*, 922−927.

(14) Moynihan, C. T.; Easteal, A. J.; Wilder, J.; Tucker, J. Dependence of the Glass Transition Temperature on Heating and Cooling Rate. *J. Phys. Chem.* **1974**, *78*, 2673−2677.

(15) Mazurin, O. V. Problems of Compatibility of the Values of Glass Transition Temperatures Published in the World Literature. *Glass Phys. Chem.* **2007**, *33*, 22−36.
(16) Barton, J. M. Dependence of Polymer Glass Transition Temperatures on Heating Rate. *Polymer* **1969**, *10*, 151−154.
(17) Pratap, A.; Singh, K.; Singh, N. L.; Shrinet, V. Heating Rate and Composition Dependence of Glass Transition Temperature of Lithium Borosulphate Glasses. *Mater. Sci. Forum* **1996**, *223*−*224*, 95−98.
(18) Grest, G. S.; Cohen, M. H. Liquid-Glass Transition: Dependence of the Glass Transition on Heating and Cooling Rates. *Phys. Rev. B: Condens. Matter Mater. Phys.* **1980**, *21*, 4113−4117.
(19) Queiroz, C. A.; Šesták, J. Aspects of the Non-crystalline State. *Eur. J. Glasses Sci. Technol. B Phys. Chem. Glasses* **2010**, *51*, 165−172.
(20) Ediger, M. D.; Angell, C. A.; Nagel, S. R. Supercooled Liquids and Glasses. *J. Phys. Chem.* **1996**, *100*, 13200−13212.
(21) Debenedetti, P. G.; Stanley, H. E. Supercooled and Glassy Water. *Phys. Today* **2003**, *56*, 40−46.
(22) Brüning, R.; Samwer, K. Glass Transition on Long Time Scales. *Phys. Rev. B: Condens. Matter Mater. Phys.* **1992**, *46*, 11318−11322.
(23) Dehaoui, A.; Issenmann, B.; Caupin, F. Viscosity of Deeply Supercooled Water and Its Coupling to Molecular Diffusion. *Proc. Natl. Acad. Sci. U.S.A.* **2015**, *112*, 12020−12025.
(24) Amann-Winkel, K.; Gainaru, C.; Handle, P. H.; Seidl, M.; Nelson, H.; Böhmer, R.; Loerting, T. Water's Second Glass Transition. *Proc. Natl. Acad. Sci. U.S.A.* **2013**, *110*, 17720−17725.
(25) Angell, C. A. Liquid Fragility and the Glass Transition in Water and Aqueous Solutions. *Chem. Rev.* **2002**, *102*, 2627−2650.
(26) Clarke, A.; Morris, G. J.; Fonseca, F.; Murray, B. J.; Acton, E.; Price, H. C. A Low Temperature Limit for Life on Earth. *PLoS One* **2013**, *8*, No. e66207.
(27) Wowk, B. Thermodynamic Aspects of Vitrification. *Cryobiology* **2010**, *60*, 11−22.
(28) Storey, K. B.; Storey, J. M. Insect cold hardiness: metabolic, gene, and protein adaptation[1]This review is part of a virtual symposium on recent advances in understanding a variety of complex regulatory processes in insect physiology and endocrinology, including development, metabolism, cold hardiness, food intake and digestion, and diuresis, through the use of omics technologies in the postgenomic era. *Can. J. Zool.* **2012**, *90*, 456−475.
(29) Junge, K.; Eicken, H.; Swanson, B. D.; Deming, J. W. Bacterial Incorporation of Leucine into Protein down to −20°c with Evidence for Potential Activity in Sub-Eutectic Saline Ice Formations. *Cryobiology* **2006**, *52*, 417−429.
(30) Heinz, J.; Krahn, T.; Schulze-Makuch, D. A New Record for Microbial Perchlorate Tolerance: Fungal Growth in NaClO4 Brines and Its Implications for Putative Life on Mars. *Life* **2020**, *10*, 53.
(31) Carr, M. H. *The Surface of Mars*; Cambridge University Press, 2007.
(32) Zhang, Y.; Nichman, L.; Spencer, P.; Jung, J. I.; Lee, A.; Heffernan, B. K.; Gold, A.; Zhang, Z.; Chen, Y.; Canagaratna, M. R.; Jayne, J. T.; Worsnop, D. R.; Onasch, T. B.; Surratt, J. D.; Chandler, D.; Davidovits, P.; Kolb, C. E. The Cooling Rate- and Volatility-Dependent Glass-Forming Properties of Organic Aerosols Measured by Broadband Dielectric Spectroscopy. *Environ. Sci. Technol.* **2019**, *53*, 12366−12378.
(33) Tu, S.; Lobanov, S. S.; Bai, J.; Zhong, H.; Gregerson, J.; Rogers, A. D.; Ehm, L.; Parise, J. B. Enhanced Formation of Solvent-Shared Ion Pairs in Aqueous Calcium Perchlorate Solution toward Saturated Concentration or Deep Supercooling Temperature and Its Effects on the Water Structure. *J. Phys. Chem. B* **2019**, *123*, 9654−9667.
(34) Toner, J. D.; Catling, D. C.; Light, B. A Revised Pitzer Model for Low-Temperature Soluble Salt Assemblages at the Phoenix Site, Mars. *Geochim. Cosmochim. Acta* **2015**, *166*, 327−343.
(35) Schawe, J. E. K.; Löffler, J. F. Existence of Multiple Critical Cooling Rates Which Generate Different Types of Monolithic Metallic Glass. *Nat. Commun.* **2019**, *10*, 1337.
(36) Johnson, W. L. Bulk Glass-Forming Metallic Alloys: Science and Technology. *MRS Bull.* **1999**, *24*, 42−56.
(37) Wang, W. H.; Dong, C.; Shek, C. H. Bulk Metallic Glasses. *Mater. Sci. Eng., R* **2004**, *44*, 45−89.
(38) Ojovan, M. Configurons: Thermodynamic Parameters and Symmetry Changes at Glass Transition. *Entropy* **2008**, *10*, 334−364.
(39) Smith, P. H.; Tamppari, L. K.; Arvidson, R. E.; Bass, D.; Blaney, D.; Boynton, W. V.; Carswell, A.; Catling, D. C.; Clark, B. C.; Duck, T.; Dejong, E.; Fisher, D.; Goetz, W.; Gunnlaugsson, H. P.; Hecht, M. H.; Hipkin, V.; Hoffman, J.; Hviid, S. F.; Keller, H. U.; Kounaves, S. P.; Lange, C. F.; Lemmon, M. T.; Madsen, M. B.; Markiewicz, W. J.; Marshall, J.; McKay, C. P.; Mellon, M. T.; Ming, D. W.; Morris, R. V.; Pike, W. T.; Rennó, N.; Staufer, U.; Stoker, C.; Taylor, P.; Whiteway, J. A.; Zent, A. P. H2O at the Phoenix landing site. *Science* **2009**, *325*, 58−61.
(40) Rennó, N. O.; Bos, B. J.; Catling, D.; Clark, B. C.; Drube, L.; Fisher, D.; Goetz, W.; Hviid, S. F.; Keller, H. U.; Kok, J. F.; Kounaves, S. P.; Leer, K.; Lemmon, M.; Madsen, M. B.; Markiewicz, W. J.; Marshall, J.; McKay, C.; Mehta, M.; Smith, M.; Zorzano, M. P.; Smith, P. H.; Stoker, C.; Young, S. M. M. Possible physical and thermodynamical evidence for liquid water at the Phoenix landing site. *J. Geophys. Res.* **2009**, *114*, No. E00E03.
(41) Cull, S. C.; Arvidson, R. E.; Catalano, J. G.; Ming, D. W.; Morris, R. V.; Mellon, M. T.; Lemmon, M. Concentrated perchlorate at the Mars Phoenix landing site: evidence for thin film liquid water on Mars. *Geophys. Res. Lett.* **2010**, *37*, L22203.
(42) Zent, A. P.; Hecht, M. H.; Cobos, D. R.; Wood, S. E.; Hudson, T. L.; Milkovich, S. M.; DeFlores, L. P.; Mellon, M. T. Initial Results from the Thermal and Electrical Conductivity Probe (TECP) on Phoenix. *J. Geophys. Res.* **2010**, *115*, No. E00E14.
(43) Martínez, G. M.; Newman, C. N.; De Vicente-Retortillo, A.; Fischer, E.; Renno, N. O.; Richardson, M. I.; Fairén, A. G.; Genzer, M.; Guzewich, S. D.; Haberle, R. M.; Harri, A.-M. .; Kemppinen, O.; Lemmon, M. T.; Smith, M. D.; de la Torre-Juárez, M.; Vasavada, A. R. The Modern Near-Surface Martian Climate: A Review of In-Situ Meteorological Data from Viking to Curiosity. *Space Sci. Rev.* **2017**, *212*, 295−338.
(44) Fischer, E.; Martínez, G. M.; Rennó, N. O. Formation and Persistence of Brine on Mars: Experimental Simulations throughout the Diurnal Cycle at the Phoenix Landing Site. *Astrobiology* **2016**, *16*, 937−948.
(45) Ahern, A. A.; Rogers, A. D.; Edwards, C. S.; Piqueux, S. Thermophysical Properties and Surface Heterogeneity of Landing Sites on Mars from Overlapping Thermal Emission Imaging System (THEMIS) Observations. *J. Geophys. Res.: Planets* **2021**, *126*, No. e2020JE006713.
(46) Lewis, S. R.; Collins, M.; Read, P. L.; Forget, F.; Hourdin, F.; Fournier, R.; Hourdin, C.; Talagrand, O.; Huot, J.-P. A Climate Database for Mars. *J. Geophys. Res.: Planets* **1999**, *104*, 24177−24194.
(47) Loerting, T.; Fuentes-Landete, V.; Handle, P. H.; Seidl, M.; Amann-Winkel, K.; Gainaru, C.; Böhmer, R. The Glass Transition in High-Density Amorphous Ice. *J. Non-Cryst. Solids* **2015**, *407*, 423−430.
(48) Fox-Powell, M.; Cousins, C. R. Partitioning of Crystalline and Amorphous Phases during Freezing of Simulated Enceladus Ocean Fluids. *J. Geophys. Res.: Planets* **2021**, *126*, No. e2020JE006628.
(49) Imrichová, K.; Veselý, L.; Gasser, T. M.; Loerting, T.; Neděla, V.; Heger, D. Vitrification and Increase of Basicity in between Ice Ih Crystals in Rapidly Frozen Dilute NaCl Aqueous Solutions. *J. Chem. Phys.* **2019**, *151*, 014503.
(50) Thomas, E. C.; Hodyss, R.; Vu, T. H.; Johnson, P.; Choukroun, M. Composition and Evolution of Frozen Chloride Brines under the Surface Conditions of Europa. *ACS Earth Space Chem.* **2017**, *1*, 14−23.
(51) Kanno, H.; Hiraishi, J. Existence of "Nearly Free" Hydrogen Bonds in Glassy Aqueous Calcium Perchlorate Solutions. *Chem. Phys. Lett.* **1981**, *83*, 452−454.
(52) Johnson, P. V.; Vu, T. H.; Hodyss, R. Crystallization Kinetics of Vitreous Magnesium Sulfate Hydrate and Implications for Europa's Surface. *Planet. Sci. J.* **2023**, *4*, 7.

(53) Hansen, G. B. Amorphous and Crystalline Ice on the Galilean Satellites: A Balance between Thermal and Radiolytic Processes. *J. Geophys. Res.* **2004**, *109*, No. E01012.
(54) Newman, S. F.; Buratti, B. J.; Brown, R. M.; Jaumann, R.; Bauer, J. M.; Momary, T. W. Photometric and Spectral Analysis of the Distribution of Crystalline and Amorphous Ices on Enceladus as Seen by Cassini. *Icarus* **2008**, *193*, 397−406.
(55) Hunt, C. J. Cryopreservation: Vitrification and Controlled Rate Cooling. *Stem Cell Banking*; *Methods in Molecular Biology*; Springer 2017; pp 41, 77.
(56) Nozawa, M.; Funaki, S.; Savela, N. Improvement of cooling rate during cryopreservation of living cells. *J. Phys.: Conf. Ser.* **2021**, *1857*, 012001.
(57) McKay, C. P.; Coustenis, A.; Samuelson, R. E.; Lemmon, M. T.; Lorenz, R. D.; Cabane, M.; Rannou, P.; Drossart, P. Physical Properties of the Organic Aerosols and Clouds on Titan. *Planet. Space Sci.* **2001**, *49*, 79−99.

https://doi.org/10.1021/acsearthspacechem.3c00090
ACS Earth Space Chem. 2023, 7, 1433−1445